IOSR Journal of Polymer and Textile Engineering (IOSR-JPTE)
e-ISSN: 2348-019X, p-ISSN: 2348-0181, Volume 3, Issue 6 (Nov. - Dec. 2016), PP 33-43
www.iosrjournals.org

Development and Property Evaluation of Poly (Lactic) Acid and Cellulose Nanocrystals Based Films with Either Silver or Peptide Antimicrobial Agents: Morphological, Permeability, Thermal, and Mechanical Characterization

Michael George, Wei-Zheng Shen, and Carlo Montemagno*
Department of Chemical and Materials Engineering University of Alberta Edmonton, Alberta T6G 2M9

Abstract: *The main aim of this paper is to report the impact of the addition of cellulose nanocrystals (CNC) on the thermal, mechanical, and permeability properties of poly (lactic acid). The thin films were prepared using a modified solvent casting method. The films were fortified with either of two antimicrobial agents: silver (Ag) nanopowder or a peptide. The microstructure, morphology, oxygen and water vapour permeability, mechanical, and thermal behaviour were investigated.It was found that thepresence of the antimicrobial agents does not adversely affect the thermal properties investigated. But, addition of greater than 0.75 % (wt.) peptide into the thin films resulted in a reduction of the mechanical properties. In all cases, there were significant reductions in oxygen and water vapour permeability. For example, for the PLA+CNC+Ag systems, there were reductions up to 50 and 40 %, respectively. The holistic interaction of the Ag nanopowder and CNC resulted in significantly better reduction in the above values. The permeability values of the studied plastics are comparable to those of commercial plastics currently on the market used for packaging.*

Keywords: *Cellulose nanocrystals, poly(lactic acid), mechanical, thermal, permeability properties*

I. Introduction

The design and manufacture of ingenious green materials from abundant renewable resources is one of the most researched themes in today's academia and industry focus. Biopolymers have been extensively researched because of their biodegradability and environmental benign nature (Heyde, 1998, Khalil et al. 2012). These materials find applications in a number of areas, inclusive of packaging materials, coating, and medicine (Fortunati et al. 2010). Poly(lactic acid) (PLA) has been one of the most innovative break through in the polymer industry. It is biodegradable, manufactured from polysaccharide sources, and exhibits desirable mechanical properties. Also, over the years, the price of this commodity has decreased significantly with improvements in process design. PLA is an attractive replacement for many of the olefin-based plastics currently dominating the market because of its similar process workability.

However, PLA is limited by its poor permeability properties and low melt point (Rhim et al. 2008, Arrieta et al. 2014). As a result, researchers have added different fillers to circumvent these shortcomings. For example, clay (Rhim et al. 2008), chitosan (Aider, 2010), microcrystalline cellulose (Fortunati et al. 2010), and cellulose nanocrystals (Fortunati et al. 2013) have been added to PLA to improve the water vapour permeability, the mechanical, and thermal properties, without compromising the transparency of the thin films. The fillers listed above are characterized with large a specific surface area that is required in order to improve the mechanical properties. But, as with any polymer, property improvement depends on the processing of the polymer into the final thin films. Specifically, extrusion and injection molding is not the best technique at the moment for PLA because of the susceptibility of the pellets to heating. Hence, in this manuscript and many previously reported (Fortunati et al. 2008, 2010), solvent casting has been used to prepare the thin films needed.
The rise of food borne related health risks associated with every day material is one major motivation for working on antimicrobial packaging materials. Silver (Ag) nanoparticles has been established as the accepted industry standard and benchmark at the moment when engineering biodegradable polymeric systems (Lloret et al. 2012). The release of silver nanoparticles in a controlled manner leads to significant antimicrobial activity against a wide array of bacteria (Falletta et al. 2008). In this manuscript, the first of two communications, the effect of Ag nanopowder or a peptide (Ppt) with antimicrobial properties was added to PLA and CNC based plastics. The effect of this specific antimicrobial peptide and its impact on the thermal, mechanical, morphological, and permeability properties of the plastics are reported. The focus is to engineer thin films with properties comparable to those of their olefin counterparts.

II. Experimental

2.1 Materials

Cellulose nanocrystals (CNC) and PLA (NatureWorks LLC, Minnetonka, USA) were obtained in-kind from a pilot scale facility at Alberta Innovates Technology Futures, Alberta, Canada. The PLA factsheet specified a glass temperature of 50-60 °C, a melt temperature of 145-170 °C, a melt density of (200°C) of 1.2 g/cc, and a pellet bulk density of 0.79-0.85 kg/L.Silver nanopowder (<100 nm, Mol. wt. 107.87 g/mol), nitric acid (70 %, Mol. wt. 63.01 g/mol), ethanol (absolute > 99.8 %, Mol. wt. 46.07 g/mol), and chloroform (anhydrous, > 99 %, Mol. wt. 119.38) were sourced from Sigma-Aldrich (Minnesota, USA).For the peptide synthesis, Fmoc-leu-OH (Mol. wt. 353.4 g/mol), Fmoc-lys(BOC)-OH (Mol. wt. 468.5 g/mol), HCTU (Mol. wt. 413.69 g/mol) were sourced from Sigma-Aldrich (Minnesota, USA). Also, Fmoc-Leu-wan resin (0.57 mmol/g, 100-200 mesh) and 4-methylmropholine (> 98 %, Mol. wt. 101.15 g/mol) were obtained from Sigma-Aldrich (Minnesota, USA).

2.2 Plastic formulations

2.2.1 CNC production

Samples of cellulose nanocrystals (CNC) were obtained from a pilot scale facility located at Alberta Innovates Technology Futures, Edmonton, Canada. The samples were stored at 4 °C until utilization. The CNC samples were obtained via hydrolysis of dissolving pulp. Reaction parameters of 120 minutes, 45 °C, stirred at 200 rpm, and a sulfuric acid concentration of 64 % (wt.) were used to produce the samples. An acid: pulp consistency of 12:1 was used for all experiments. Samples were finally spray dried for transport and storage.

2.2.2 Peptide synthesis

E14LKK is a 14 residue, magainin-class peptide with broad-spectrum demonstrated antimicrobial activity (Steven and Hotchkiss, 2008). It was synthesized by following the standard Fmoc (9-fluroenylmethoxycarbonyl)-based solid-phase peptide synthesis (SPPS) protocol (Fields and Noble, 1994). The freeze-dried peptide was re-suspended before addition to the plastics. A structural representation of the peptide is provided below in Scheme 1.

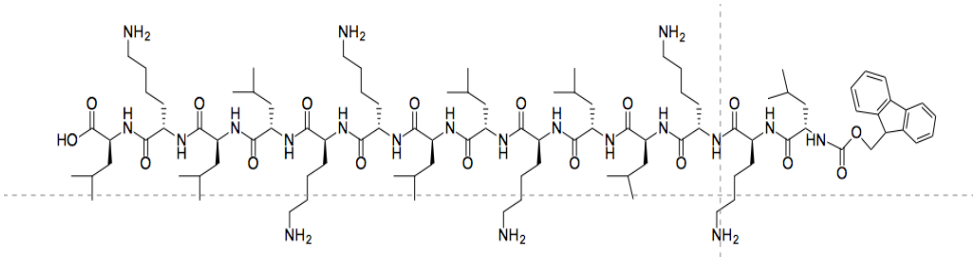

Scheme 1. Representation of the synthesized peptide antimicrobial agent

2.2.3 Experimental design for thin film production

Thin films were made from PLA and CNC. Solvent casting was used to produce all films. Plastics were fitted with silver nanoparticles or the peptide. The experimental design is presented in Table 1.

Table 1. Experimental design

System	Wt. PLA (mg)	Wt. CNC (%)	Wt. Ag (%) or Peptide (%)[1]
PLA[2]	1000 mg	-	-
PLA_CNC_1.0%CNC	980 mg	1.0	-
PLA_CNC_2.5%CNC	975 mg	2.5	-
PLA_CNC_5.0%CNC	950 mg	5.0	-
PLA_CNC_1.0%CNC_xAg	980 mg	1.0	0.25, 0.75, 1.25
PLA_CNC_2.5%CNC_xAg	975 mg	2.5	0.25, 0.75, 1.25
PLA_CNC_5.0%CNC_xAg	950 mg	5.0	0.25, 0.75, 1.25

[1] Given these components were used in such low weight relative to CNC and PLA, they were not calculated into the final weight.
[2] Control for CNC based PLA plastics

As can be appreciated, many films were formulated because of the number of parameters covered. For any given system, the required amount of PLA was dissolved in 20 mL chloroform and stirred for 2 hours. Depending on the system, a specific amount of CNC (and in some cases either Ag or peptide) were weighed separately and slowly added to the PLA on the stir plate. The sample was vigorously stirred for another 2 hours

(4 hours when Ag or peptides were added). Immediately after stirring, the PLA mix was poured onto a Pyrex 9 cm petri dish (all sample types were done in triplicate). A smooth stirring rod was used to evenly distribute the PLA mix onto the bottom of the petri dish. All petri dishes were covered with aluminium foil (holds were punctured on the top to allow chloroform to evaporate) to facilitate slow evaporation of chloroform in a fume hood. After 24 hours (36 hours in some instances, when peptides were used), the plastics were peeled from the bottom of the dishes and conditioned in a vacuum over at 40 °C for 8 hours. Samples were sealed in bags and stored for subsequent analysis.

2.3 Characterization of plastics

2.3.1 Morphological study-SEM

Samples that exhibited improved properties and in some case no change were randomly selected for morphological study. Cross-sectional images were taken using a Zeiss Sigma Field Emission Scanning Electron Microscope (FE SEM) equipped with an Everhart-Thornley Secondary Electron detector (ET-SE). Images were taken at an accelerating voltage of 5 kV and a maximum resolution at 1.5 nm. Prior to analysis, a gold sputter coater was using to coat all samples, to induce conductivity. In most cases, 3 pieces of film were randomly selected from the failed pieces obtained from mechanical testing.

2.3.2 Oxygen transmission rate (OTR)

The OTR for the different plastic systems were measured using an oxygen permeation analyser (SYSTECH Illinois Instruments, model 9500, IL, USA). The instrument was equipped with a zirconia solid state-measuring cell. Plastic samples were cut to a diameter of 15 cm for each test. The thickness of the films was determined using a micrometre. The sample was clamped in the diffusion chamber, which was maintained at 25 ± 1 °C. Oxygen was introduced into the upper half of the chamber while nitrogen was injected into the lower half, where an oxygen sensor was kept. To ensure reproducibility, five samplesper plastic type were tested.

2.3.3 Water vapour permeability (WVP)

The water vapour permeability of plastics is an important parameter when manufacturing plastics for food packaging. In this study, the WVP was determined according to ASTM E96/E96M-Standard Test Methods for Water Vapour Transmission of Materials. According to the standard, MVP can be defined as the time rate of water vapour transmission through an unit area of flat materials of unit thickness induced by the unit vapour pressure differences between two specific surface, under specified temperature and humidity conditions.

For most experiments, 80 mm diameter samples were carefully fixed to test dishes that were filled ¼ with distilled water. The dish assembly was weighted and placed in the controlled conditioning chamber maintained at 50 ± 2 % relative humidity and 20 ± 0.5 °C. A dummy specimen (no water in test dish) was done parallel to all experimental samples. This dummy specimen will account for the environmental fluctuations in temperature, humidity, and weighing. The weights of the different sample dishes were taken at least at 8 time points to facilitate the construct of a line graph (variation of weight gain with time). The weighing of dishes was done in the controlled environment. For a given sample, linear regression was used to estimate the slope of the lines of the individual samples.

The first stage of the numerical analysis involved calculating the water vapour transmittance (MVT) as given in equation 1:

$$WVT = \frac{G}{tA} = {\left(\frac{G}{t}\right)}\Big/{A}$$

where:

G = weight change (from straight line), g,

t =time, h,

G/t = slope of the straight line, g/h,

A = test area (dish mouth size), m^2

WVT = rate of water vapour transmission, g/h*m^2

The permeability of the films were calculated using equation 2:

$$WVP = \frac{WVT}{\Delta P} = \frac{WVT}{S}(R_1 - R_2)$$

where:

ΔP = vapour difference, mm Hg

S = saturation vapour pressure at test temperatures

R_1 = relative humidity of chamber

R_2 = relative humidity inside the test dish

It should be noted, in cases where the film thickness was < 0.02 mm, the WVP was multiplied by actual film thickness (mm). Three repetitions were performed per sample type.

2.3.4 Thermal properties

The effect of the different formulations on the thermal stability of was investigated using Thermal gravimetric analysis (TGA). All samples were tested using a Thermal Analysis Instruments TGA Q50 (TA Instruments) apparatus under a flow of nitrogen to study the effects of heating on stability of the different thin films. Platinum pans were used given the high temperatures and the ease of cleaning. The temperature range selected was from room temperature to 600 °C at a rate of 10 °C increase per minute. Triplicate runs were done for each level per treatment. All results were reproduced to 5 % error or better.
Differential scanning calorimetry (DSC) was used to investigate the thermal transitions for each sample. These measurements were performed using a Thermal Analysis Instruments DSC Q2000 (TA Instruments) in the temperature range of 25-300 °C at a heating rate of 10 °C per minute. Approximately 5-10 mg of sample was used for each analysis. For each sample, triplicate runs were done.

2.3.5 Mechanical property evaluation

For all mechanical testing, an Instron dual column table-top universal testing (System 3365) equipped with a 5 kN capacity, 1000 mm/min maximum crosshead speed, and vertical test space of 1192 mm was used. Prior to testing, all samples were conditioned at 40 °C for 8 hours. Depending on the precision of the measurements, up to 8 tests were done for each sample.Cast films were cut into 5 by 50 mm pieces. The thickness, ranging from 65 to 90 μm, was determined using a micrometer. For samples, where the thickness was < 65 μm, an assumption was made that the thickness was 65 μm. A head speed of 10 mm/min was used for all measurements. The tensile measurements were conducted according to ASTM D 882 Standard Test Method for the tensile properties of thin plastic sheeting.

2.3.6 X-ray diffraction investigation

All experiments were carried out on a Bruker-AXS, D8 discover diffractometer system equipped with a Vantec-500 area detector and Cu Kα1 radiation source ((λ = 1.542 A). The instrument was operated at 40 kV and 30 mA for x-ray diffraction (XRD) experiments. The XRD patterns were obtained by irradiating the films from phi=00 ~ 180 ° over the angular range of 2θ = 5 ~ 80 ° for 300 seconds. XRD patterns of the different thin films were examined. Peak deconvolution method was used to distinguish the CNC peaks and other peaks in XRD spectra, as previously reported by Hamad and Hu (2010). The curve fitting procedure required assumptions about the shape and number of peaks. CNC's diffraction peaks was assigned to 2θ = 16.5, 22.5, 34.6, which are characteristic for planes 110, 200, and 400 (Godinho et al. 2014, Guang et al. 2015).

2.4 Statistical analysis

All experiments were replicated at least three times and the results are expressed as mean value ± standard deviation. Statistical analysis was done using SAS Version 9.4. All data sets that were normally distributed were analysed using t-test embedded in Microsoft Excel. For those systems that were not normally distributed, to identify significant differences the Kruskal Wallis Test was applied to the data populations involved, with a 95% confidence level ($P < 0.05$).

III. Results And Discussion

3.1 Morphological properties

Scanning electron micrographs were taken of virgin and fractured (via tensile testing) PLA and CNC based plastics. These images are presented in Fig 1. The PLA + CNC micrograph was characterized with irregularsurface patterns, as previously reported by Fortunati et al. (2012). Further, when the antimicrobial agents were introduced into the PLA plastic, the surfaces of the plastics were characterized with increased roughness, resulting from a "layered" like structure. Careful observation of the lower left panel in Figure 1 indicates that during the solvent casting processing, more than one layer of plastic resulted. This phenomenon has not been previously highlighted or reported and plausibly resulted from the agglomeration of the CNC in the solvent used, which can cause stacking of the PLA polymer, instead of a flat and smooth plastic. The fractured CNC + PLA plastic sample was studied to observe any agglomeration of CNC within the macrostructure of the plastic. As evident, there were no major voids or agglomerated areas of the studied plastics, pointing to good dispersion of CNC within the matrix.

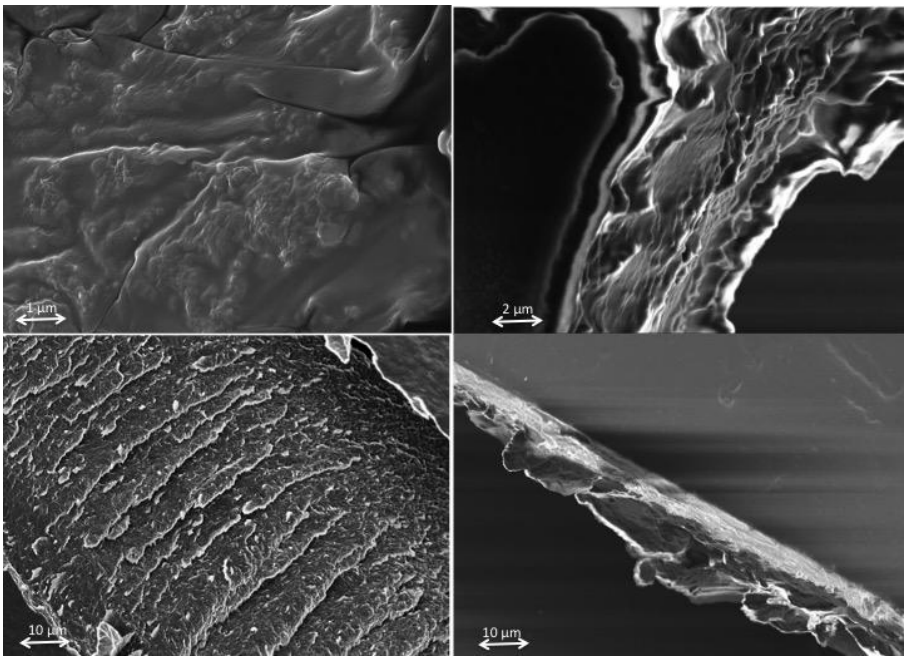

Figure 1. Micrographs of PLA + CNC (upper left panel), PLA + CNC + peptide (upper right panel), PLA + CNC + Ag (lower left panel) and PLA + CNC fractured plastics (lower right panel

3.2 Permeability study

3.2.1 Water vapour permeability (WVP)

The water vapour permeability (WVP) measurements for the different PLA based systems are given in Table 2. Further, the % reduction of the WVP of the PLA+CNC+Ag/Ppt plastics when compared to the PLA+Ag/Ppt (controls-absence of CNC) plastics are presented in Fig2.

Table 2. Water vapour permeability coefficients for the different PLA based plastics

System	**Type of antimicrobial agent – water vapour permeability (WVP*10^{14} – kg mm^{-2} s^{-1} Pa^{-1})**							
	Ag (%)				**Ppt (%)**			
	0	**0.25**	**0.75**	**1.25**	**0**	**0.25**	**0.75**	**1.25**
PLA	1.27/0.15	1.21/0.31	1.08/0.08	1.12/0.14	1.11/0.13	1.14/0.21	1.28/0.38	1.02/0.18
PLA+1% CNC	1.09/0.04	1.01/0.10	0.90/0.07	0.89/0.01	1.01/0.24	1.03/0.11	1.21/0.24	0.97/0.03
PLA+2.5% CNC	0.85/0.02	0.78/0.17	0.71/0.03	0.73/0.07	0.99/0.04	1.01/0.11	1.19/0.06	0.90/0.12
PLA+5% CNC	0.78/0.10	0.79/0.05	0.74/0.03	0.73/0.09	1.14/0.11	1.09/0.06	0.96/0.09	0.99/0.12

Note: Systems with CNC and or Ag/Ppt. were compared to their counterpart PLA or PLA + AG or PLA + Ppt. and not at the different Ag or Ppt. levels. Results presented as mean/SD.

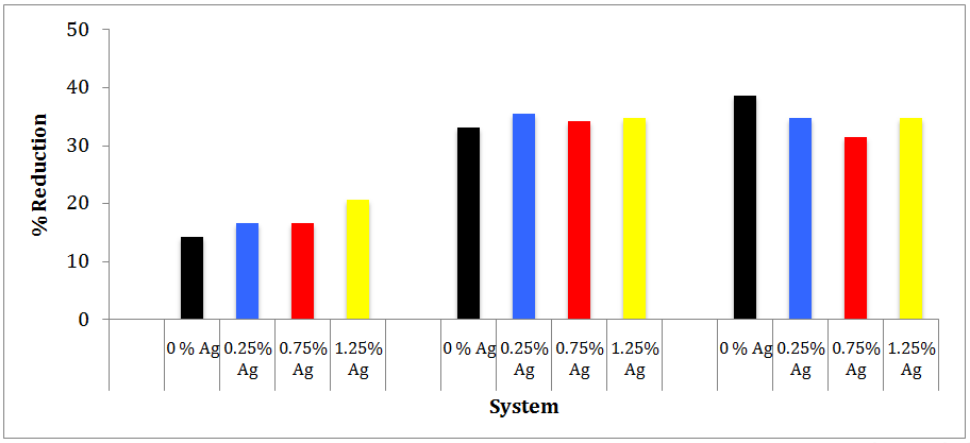

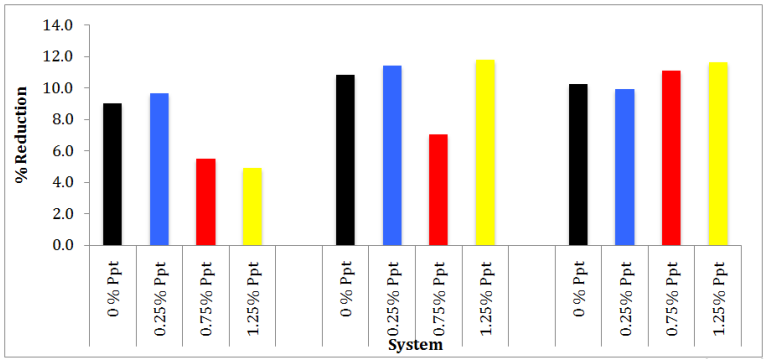

Figure 2. Representation of the % reduction for the two major systems, Ag nanopoweder (upper panel) and peptide based PLA plastics (lower panel)

There was significant reduction in the WVP of the different systems when CNC was added. In fact, systems with both CNC and Ag nanoparticles were characterized with up to 40 % reduction in the WVP when compared to the control sample (PLA, or PLA with Ag nanopowder). From the results, it is clear that the WVP reduction reaches a threshold when 2.5 % of CNC is added to the PLA plastics. That is, with addition of 5 % CNC to the PLA, at varying Ag powder or peptide, there was no major differences between the 2.5 % and 5 % CNC systems. When compared to a study reported by Fortunati et al. (2012), where they engineered PLA based plastics with unmodified and modified CNC, it was found that our results are comparable with the modified CNC system they reported. Additionally, the correlation between % CNC added and % reduction in WVP was previously reported by Sanchez-Garcia et al. (2008) when they found that addition of 1 % CNC resulted in 10 % reduction, but there was no difference after 2 or 3 % of CNC were added.

When compared, the addition of the different antimicrobial agents (Ag versus Ppt), it was found that the Ag nanopowder significantly outperformed its peptide counterpart. In fact, the Ag based systems were characterized with at least 30 % more reduction than the peptide-based plastics. To better understand what caused this observation, one has to fully understand the factors at play when measuring the WVP. Additionally, what factors influence the end results are just as important. It has been previously reported that the transport properties of gases through polymeric films are significantly influenced by the tortuosity of the gases path, which depends on the shape and aspect ratio of the filler, the degree of dispersion, % filler loading, orientation of the filler, and polymer chain immobilization (Sanchez-Garcia et al. 2008). Hence, it is not surprising that the nanopowder outperformed its peptide counterpart. Firstly, the former is characterized by nano dimensions and will readily be more evenly dispersed within the PLA. Also, the peptides were found to be difficult to disperse in the chloroform media used. As a result, in some cases, the peptide based films it was clear that the dispersion of the peptides within the casted films was not uniform. Also, there seems to be a synergistic effect between the Ag and CNC nanoparticles, which holistically leads to the reduction in the WVP. These observations alone, can account for major differences between the two systems.

In summary, the engineering PLA based plastics were characterized with significant reduction in their WVP. This is a move in the right direction if these plastics are to be considered as food packaging materials.

3.2.2 Oxygen Transmission Rate (OTR)

All CNC reinforced PLA based films were characterized with significant reduction in their OTR when compared to the controls. The exact calculated OTR values are presented in Table 3 while the % reduction for each system is highlighted in Fig 3. As evident from SEM imaging, the uniform distribution of CNC within the PLA structure facilitated the reduction in the OTR. Also, addition of Ag nanopowder was better at lowering the OTR when compared to the peptide based plastics. The plausible reason for this can be linked back to the discussion had earlier in section 3.2.1. The holistic effect of the CNC and Ag nanoparticles resulted in better dispersion and orientation within the PLA matrix.

Table 3. Oxygen transmission rate for the different PLA based plastics

System	**Type of antimicrobial agent – oxygen transmission rate (OTR $cm^3*mm*m^{-2}*day^{-1}$)**							
	Ag (%)				**Ppt (%)**			
	0	**0.25**	**0.75**	**1.25**	**0**	**0.25**	**0.75**	**1.25**
PLA	32.7/2.3	32.5/0.8	31.8/3.5	31.5/2.9	29.8/3.1	28.0/1.9	27.9/3.6	29.1/1.3
PLA+1% CNC	21.4/0/5	19.9/0.9	20.5/1.1	20.9/0.4	25.4/0.4	23.6/1.4	23.9/2.9	24.9/0.8
PLA+2.5% CNC	18.2/1.	18.7/2.	16.9/0.	17.7/0.	24.0/1.	22.4/0.	23.1/0.	23.5/3.

	3	4	3	7	3	3	7	8
PLA+5% CNC	17.8/1.2	18.1/0.8	16.3/2.8	17.2/3.9	23.3/3.1	21.4/1.9	22.1/1.1	23.2/0/7

Resulted presented as mean/SD.

The values presented in Table 3 are lower than those presented by Colomines et al. (2008) when they studied the influence of the crystallization rate on the thermal and barrier properties of PLA packaging films. A few key differences in these studies was that their studied focused on extruding the plastics while we solvent casted. Also, the sources of the PLA used were different between studies. Nevertheless, the values obtained in this study are significantly lower than those they reported for their PLA plastics and even for conventional plastics such as low-density polyethylene and polystyrene. As presented in the previous section, the % OTR values were calculated based on comparing against the plastics without CNC. Żenkiewicz and Richert (2008) investigated the influence of two types of montmorillonite nanofillers (Cloisite 30B and Nanofil 2), two kinds of organic modifiers (polymethyl methacrylate and ethylene/vinyl alchohol copolymer), and two types of compatibilizers (polycaprolactone and poly(ethyleneglycol)) on the transmission rate of oxygen through PLA films. Interestingly, they found that PLA plastics with organic modifiers were characterized with reduced oxygen transmission rates. In fact, a plastic system with 75, 20, and 5 % (wt.) of PLA, polymethyl methacrylate, and Cloisite 30 B, respectively, was characterized with a 55 % reduction in the oxygen transmission rate when compared to the virgin PLA plastics. As a result, the values presented in Figure 3 are very encouraging because in this study, a very low concentration of CNC (nanofiller) was added, when compared to the study outlined above. Nevertheless, we were able to obtain reductions up to 45 % for PLA + CNC + Ag nanopowder and 20 % for PLA + CNC + Ppt. plastics. This points to the plausible conclusion that CNC is a better nanofiller when it comes to dispersion within the matrix and is better at reducing the amorphous phase of the polymer (the amorphous phase is responsible for gas permeation).

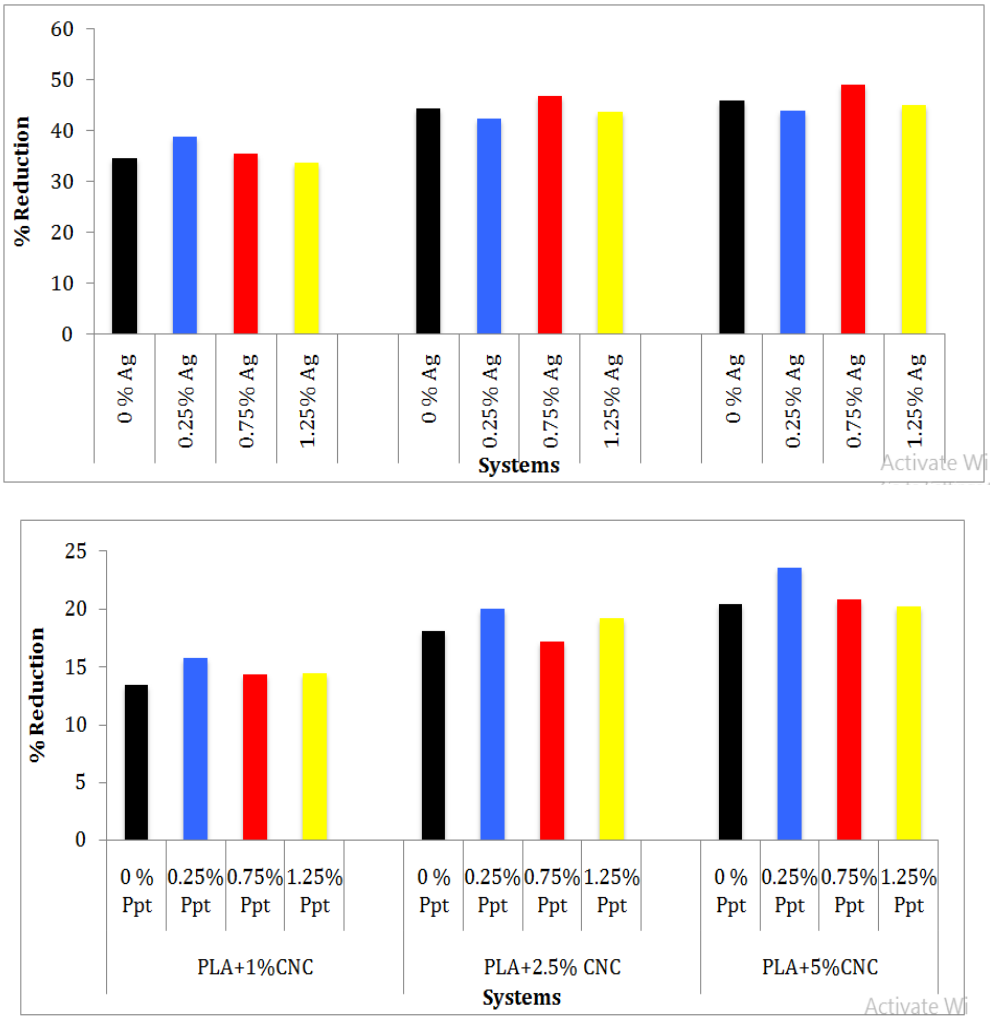

Figure 3. Representation of the % reduction for the two major systems, Ag nanopoweder (upper panel) and peptide based PLA plastics (lower panel)

3.3 Thermal properties

The thermal properties of the different PLA based formulations were investigated using Thermal gravimetric analysis (TGA) and Differential scanning calorimetry (DSC). DSC was used to estimate the glass transition temperature and the melting endotherm of the different thin films. The respective results for Ag based films and peptide (Ppt) based films are given in Table 4 and 5, respectively. PLA with CNC was characterized with significant improvement in degradation when considering the temperature needed to degrade 10 % of each sample. The results are promising because when Fortunati et al. (2010) reinforced PLA with MCC, they saw a decrease of 10 °C for most of the PLA + CNC systems. One plausible reason for the improved degradation pattern observed in this study may have been because of the uniform particle distribution and the superior temperature degradation of CNC, when compared to MCC. Interestingly, thermographs for the PLA reinforced with CNC were characterized with two major peaks, within the 20 % degradation temperature. In fact, higher the concentration of the CNC added to the PLA plastics, the trend became clearer. According to Fortunati et al. (2010), the first peak (around 325-330 °C) is characteristic of disruption of the hydrogen bonding among the CNC network. On the other hand, the other peak (around 340-348 °C) was attributed to the depolymerisation of the PLA matrix. These trends were expected because CNC degrades before the matrix.

The PLA + CNC (with or without antimicrobial agent) were characterized with glass transition and melting endotherms similar to those reported by Fortunati et al. (2010). But, when 1.25 % Ag or peptide was added, the plastics were characterized with a reduction in the glass transition temperature. In theory, the glass transition is the energy needed to make a system go from a rigid material to a rubbery state. In most instances, several factors are integral to determine the reasons for reductions as observed. One plausible reason in this case could have been the poor dispersion of the antimicrobial agents as its concentration increase. To that end, higher the concentration, higher the chances of introducing flaws within the structure, which can significantly impact the glass transition temperature. In summary, PLA+CNC+Ag/Ppt plastics were characterized with improved thermal resistance as the concentration of CNC increased in the films. Also, high concentration of antimicrobial agents resulted in reduction of the glass transition temperatures. As will be explained in the following section, another reason for the improved thermal properties could have been the increased crystallinity brought on by the addition of CNC.

Table 4. Thermal properties of the different Ag based PLA and CNC films

Sample	Sub-sample	Tg (°C)	Melting endotherm (Tm)	Temp. 10 % degradation	Temp. 20 % degradation
PLA	0% Ag	52.9 / 2.35	150.3 / 1.99	327.4 / 3.68	337.1 / 4.29
	0.25% Ag	52.8 / 3.91	148.3 / 4.88	330.2 / 5.33	329.4 / 10.6
	0.75% Ag	51.4 / 6.34	140.5 / 9.33	319.4 / 5.99	325.4 / 5.39
	1.25% Ag	52.3 / 4.23	142.5 / 2.53	324.7 / 6.90	320.3 / 4.99
PLA+1%CNC	0% Ag	55.1 / 0.45	154.8 / 0.56	332.3 / 5.13	350.0 / 6.20
	0.25% Ag	54.8 / 2.60	156.8 / 2.43	332.3 / 1.53	346.0 / 4.00
	0.75% Ag	52.2 / 2.21	155.2 / 1.75	344.7 / 3.51	349.7 / 5.69
	1.25% Ag	53.2 / 1.17	158.6 / 0.71	343.3 / 2.52	350.0 / 4.58
PLA+2.5% CNC	0% Ag	53.7 / 0.57	154.5 / 0.72	343.0 / 2.64	344.0 / 3.61
	0.25% Ag	55.0 / 1.31	157.7 / 2.12	343.3 / 4.99	347.3 / 1.53
	0.75% Ag	55.0 / 2.51	153.8 / 2.51	341.7 / 2.08	347.0 / 1.00
	1.25% Ag	54.4 / 1.70	153.2 / 2.18	343.7 / 1.53	354.0 / 5.00
PLA+5%CNC	0% Ag	52.3 / 0.72	147.3 / 1.51	346.0 / 2.65	345.0 / 4.00
	0.25% Ag	51.4 / 0.49	150.3 / 3.21	343.7 / 2.52	346.3 / 2.52
	0.75% Ag	52.6 / 1.30	148.4 / 0.93	340.7 / 1.53	349.0 / 2.08
	1.25% Ag	48.3 / 0.85	149.9 / 1.15	344.7 / 2.08	352.3 / 4.16

Table 5. Thermal properties of the different peptide (Ppt) based PLA and CNC films

Sample	Sub-sample	Tg (°C)	Melting endotherm (Tm)	Temp. 10 % degradation	Temp. 20 % degradation
PLA	0% Ppt	52.9 / 2.35	153.3 / 1.49	323.1 / 3.91	338.3 / 2.59
	0.25% Ppt	49.8 / 4.85	145.3 / 9.88	329.4 / 6.39	334.1 / 2.06
	0.75% Ppt	50.4 / 2.14	144.5 / 4.49	321.1 / 2.09	327.3 / 2.19
	1.25% Ppt	50.0 / 1.23	146.1 / 3.53	323.6 / 1.40	328.1 / 1.04
PLA+1%CNC	0% Ppt	54.2 / 0.17	153.8 / 1.06	334.3 / 2.93	341.4 / 2.90
	0.25% Ppt	54.9 / 0.65	159.9 / 2.71	335.1 / 0.51	340.1 / 3.80
	0.75% Ppt	51.1 / 0.29	158.1 / 2.35	338.5 / 1.99	344.3 / 2.99
	1.25% Ppt	54.9 / 1.47	159.7 / 1.70	341.1 / 1.02	349.1/ 4.18
PLA+2.5% CNC	0% Ppt	54.1 / 1.52	155.1 / 1.32	335.0 / 1.69	341.0 / 4.21
	0.25% Ppt	51.4 / 0.91	152.8 / 2.91	338.1 / 3.09	343.5 / 1.93
	0.75% Ppt	53.0 / 1.56	154.8 / 3.79	341.9 / 6.08	344.0 / 1.40
	1.25% Ppt	53.9 / 2.50	154.4 / 3.10	339.7 / 5.51	346.0 / 3.30

PLA+5%CNC	0% Ppt	54.1 / 1.72	146.1 / 2.51	338.0 / 1.62	344.0 / 0.09
	0.25% Ppt	52.9 / 1.41	148.3 / 2.01	341.7 / 0.52	344.1 / 0.59
	0.75% Ppt	53.9 / 1.90	146.7 / 0.13	340.5 / 1.10	347.4 / 1.98
	1.25% Ppt	49.3 / 1.89	149.1 / 3.16	344.3 / 1.18	351.3 / 1.99

3.4 Mechanical properties

The mechanical properties of the different PLA based plastics are presented in Table 6 and 7. When CNC was added to PLA, at different concentrations, there was a corresponding increase in the tensile strength and the Young's Modulus of the films. The only exception being significant decreases when greater than 0.75 % of peptide was added to the films. In these cases, the plastics were characterized with rapid failure and in some instances, ripping during testing. Plausible reasons for this include increased cracks and flaws in the plastic's macrostructure as the concentration of peptide increases. Nevertheless, addition of 0.25 and 0.75 % of the peptide produced plastics with improved properties. The reduction of the elongation at break with the addition of CNC and the antimicrobial agent is a common trend observed in the literature (Sain et al. 2004 and Sanjay et al. 2015). This results from the introduction of the filler that causes the formation of stress concentrations along the film. On the other hand, a few systems (peptide based) were characterized with significant increases in elongation. Careful observation of these systems would highlight a corresponding decrease in the Modulus. Hence, the introduction of flaws within the structure resulted in better slippage of the different layers of the film.

Table 6. Mechanical properties of the different Ag based PLA and CNC films

Sample	Sub-sample	Tensile strength (MPa)	Modulus (MPa)	% Elongation
PLA	0 % Ag	19.4 / 0.51	2514 / 212	6.14 / 0.20
	0.25% Ag	17.5 / 1.47	2468 / 108	6.02 / 0.58
	0.75% Ag	20.1 / 0.89	2399 / 130	6.59 / 1.05
	1.25% Ag	21.3 / 1.91	2601 / 101	6.16 / 1.53
PLA+1%CNC	0 % Ag	17.5 / 1.47	2645/ 39	4.48 / 0.33
	0.25% Ag	18.7 / 0.39	2659 / 166	4.99 / 0.21
	0.75% Ag	17.4 / 0.64	2681 / 200	4.98 / 0.32
	1.25% Ag	17.6 / 0.70	2687 / 87	5.12 / 0.41
PLA+2.5% CNC	0 % Ag	22.1 / 0.80	2700 / 33	4.55 / 1.05
	0.25% Ag	21.5 / 1.74	2711 / 22	4.79 / 0.42
	0.75% Ag	22.9 / 0.70	2696 / 131	5.38 / 0.33
	1.25% Ag	22.3 / 0.69	2721 / 37	4.20 / 0.20
PLA+5%CNC	0 % Ag	23.1 / 1.11	2864 / 24	5.10 / 0.53
	0.25% Ag	23.3 / 0.75	2899 / 45	4.86 / 0.30
	0.75% Ag	22.7 / 0.64	2985 / 26	5.04 / 0.34
	1.25% Ag	24.1 / 1.03	2946 / 20	5.14 / 0.26

Table 7. Mechanical properties of the different peptide (Ppt) based PLA and CNC films

Sample	Sub-sample	Tensile strength (MPa)	Modulus (MPa)	% Elongation
PLA	0 % Ppt	19.2 / 0.41	2396 / 29	5.99 / 0.41
	0.25% Ppt	16.5 / 3.47	2315 / 41	6.09 / 0.28
	0.75% Ppt	17.1 / 1.85	2360 / 98	6.79 / 1.41
	1.25% Ppt	18.3 / 4.91	2348 / 74	6.56 / 2.53
PLA+1%CNC	0 % Ppt	19.5 / 1.07	2395 / 21	6.02 / 0.63
	0.25% Ppt	18.7 / 0.39	2559 / 46	5.94 / 0.21
	0.75% Ppt	19.4 / 2.34	2349 / 20	6.90 / 2.32
	1.25% Ppt	17.1 / 3.70	2499 / 37	6.92 / 0.09
PLA+2.5% CNC	0 % Ppt	22.4 / 0.60	2511 / 31	6.59 / 0.59
	0.25% Ppt	20.1 / 1.34	2601 / 84	6.71 / 0.22
	0.75% Ppt	19.3 / 0.24	2649 / 36	6.45 / 0.23
	1.25% Ppt	15.3 / 0.39	2224 / 17	9.20 / 0.41
PLA+5%CNC	0 % Ppt	22.1 / 0.21	2844 / 29	5.46 / 0.13
	0.25% Ppt	22.3 / 0.49	2817 / 15	5.09 / 1.09
	0.75% Ppt	18.0 / 0.29	2605 / 46	5.99 / 0.54
	1.25% Ppt	16.1 / 0.73	2536 / 29	6.31 / 0.27

Values in red are against any trends observed (when compared to the system with no CNC).Values represented as mean / SD.

In the end, PLA + 5 % CNC with any given concentration of Ag nanopowder produced films with the highest tensile strength and Young's Modulus. It was also observed that addition of high concentration of peptide to the films adversely affected the mechanical properties. But, in cases, where high elongation at break is integral, these systems can be adopted.

3.5 X-ray diffraction study

The crystal structure of PLA, PLA+CNC, PLA+CNC+Ag, and PLA+CNC+Ppt were characterized by x-ray scattering in order to study the effect of the nanocrystal addition, influence of the antimicrobial agents, and additive behaviour of both. Fig 4 shows the x-ray diffraction pattern for the different plastic samples.

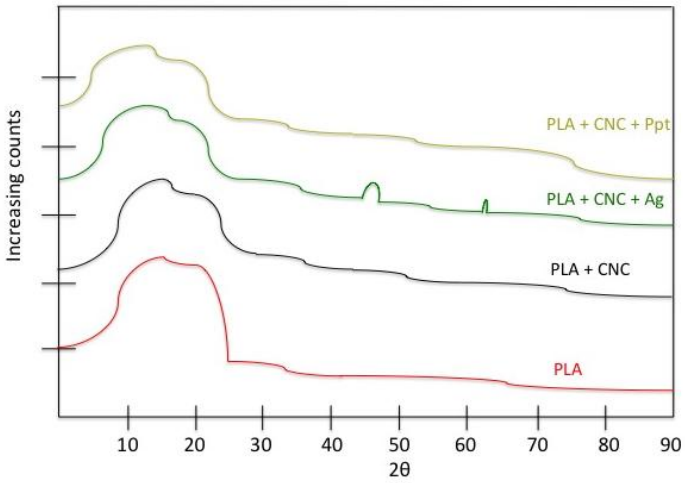

Figure 4. XRD patterns of the different samples types investigated

All PLA based plastics were characterized with a broad diffraction band at 2θ = 16.5 °, consistent with the amorphous structure of PLA. When CNC was introduced into the plastics, a peak characteristic of the cellulosic crystallinity appeared at 2θ = 22.5 ° (Sullivan et al. 2015). It should be noted that these samples contained 1 % (w/w) of CNC, hence the reason why the crystallinty peak was not obvious. For the Ag based films, peaks at approximately 2θ = 38 and 63 ° are characteristic of Ag crystals. These crystals correspond to the diffraction planes of (111) and (220), respectively (Fortunati et al. 2013). The presence of these peaks conclusively implies that the Ag nanoparticles were embedded into the PLA+CNC based plastics. Finally, the PLA+CNC+Ppt was characterized with peaks characteristic of PLA and CNC. No peaks appeared because of the presence of the peptide.It should be noted, the % crystallinity was not determined because of the low concentration of CNC added to the PLA matrix. That is, the addition of the concentrations outlined in this communication will not significantly change the crystallinity index of the plastics. Nevertheless, it was imperative that the patterns of the different systems be presented to provide evidence that the Ag nanopowder or peptide was embedded into the PLA matrix.

IV. Conclusions

The manufacture and characterization of nano-based thin films using poly(lactic) acid for food packaging applications using a combination of cellulose nanocrystals and either silver or a peptide based antimicrobial agent was carried out. Scanning electron micrographs demonstrated that the dispersion of the CNC and or the antimicrobial agents within the film significantly affected the thermal and mechanical properties. Poly(lactic) acid with 5 % CNC and the silver antimicrobial agent based films were characterized with significantly improvements in mechanical properties and increased thermal resistance. These are very attractive properties for producing films for packaging materials. Nevertheless, in cases where greater than 0.75 % of the peptide was introduced, reductions in the above values were observed. Finally, most films with CNC and the antimicrobial agents were characterized with significantly improved oxygen and water permeability properties, making them competitive with olefin-based plastics currently dominating the market. In the end, from this work, we have produced nano-reinforced poly(lactic) acid plastics with comparable thermal and mechanical properties and they can be used as a green alternative to current film formulations of food packaging. The next phase of the project builds on evaluating the migration properties and the antimicrobial effects of the different studies.

Acknowledgements

This work could not have been possible without the funding provided by the Government of Alberta. The assistance of Dr. He, attached to nanoFab, of the University of Alberta is much appreciated.

References

[1] Abdul Khalil, H. P. S., Bhat, A. H., & Ireana Yusra, A. F. (2012). Green composites from sustainable cellulose nanofibrils: A review. Carbohydrate Polymers,87(2), 963-979. doi:http://dx.doi.org/10.1016/j.carbpol.2011.08.078

[2] Aider, M. (2010). Chitosan application for active bio-based films production and potential in the food industry: Review. LWT - Food Science and Technology,43(6), 837-842. doi:http://dx.doi.org/10.1016/j.lwt.2010.01.021

[3] Arrieta, M. P., Fortunati, E., Dominici, F., López, J., & Kenny, J. M. (2015). Bionanocomposite films based on plasticized PLA–PHB/cellulose nanocrystal blends.Carbohydrate Polymers, 121, 265-275. doi:http://dx.doi.org/10.1016/j.carbpol.2014.12.056
[4] Chung, D., Papadakis, S. E., & Yam, K. L. (2002). Simple models for assessing migration from food-packaging films. Food Additives and Contaminants, 19(6), 611-617. doi:10.1080/02652030210126389
[5] Colomines, G., Domenek, S., Ducruet, V., & Guinault, A. (2008). Influences of the crystallisation rate on thermal and barrier properties of polylactide acid (PLA) food packaging films. International Journal of Material Forming, 1, 607-609. doi:10.1007/s12289-008-0329-0
[6] FIELDS, G., & NOBLE, R. (1990). Solid-phase peptide-synthesis utilizing 9-fluorenylmethoxycarbonyl amino-acids. International Journal of Peptide and Protein Research, 35(3), 161-214.
[7] Fortunati, E., Armentano, I., Iannoni, A., & Kenny, J. M. (2010). Development and thermal behaviour of ternary PLA matrix composites. Polymer Degradation and Stability, 95(11), 2200-2206. doi:http://dx.doi.org/10.1016/j.polymdegradstab.2010.02.034
[8] Fortunati, E., Peltzer, M., Armentano, I., Jiménez, A., & Kenny, J. M. (2013). Combined effects of cellulose nanocrystals and silver nanoparticles on the barrier and migration properties of PLA nano-biocomposites. Journal of Food Engineering, 118(1), 117-124. doi:http://dx.doi.org/10.1016/j.jfoodeng.2013.03.025
[9] Fortunati, E., Peltzer, M., Armentano, I., Jiménez, A., & Kenny, J. M. (2013). Combined effects of cellulose nanocrystals and silver nanoparticles on the barrier and migration properties of PLA nano-biocomposites. Journal of Food Engineering, 118(1), 117-124. doi:http://dx.doi.org/10.1016/j.jfoodeng.2013.03.025
[10] Fortunati, E., Peltzer, M., Armentano, I., Torre, L., Jiménez, A., & Kenny, J. M. (2012). Effects of modified cellulose nanocrystals on the barrier and migration properties of PLA nano-biocomposites. Carbohydrate Polymers, 90(2), 948-956. doi:http://dx.doi.org/10.1016/j.carbpol.2012.06.025
[11] Godinho, M. H., Almeida, P. L., & Figueirinhas, J. L. (2014). From cellulosic based liquid crystalline sheared solutions to 1D and 2D soft materials. Materials,7(6), 4601-4627. doi:10.3390/ma7064601
[12] Guang, S., An, Y., Ke, F., Zhao, D., Shen, Y., & Xu, H. (2015). Chitosan/silk fibroin composite scaffolds for wound dressing. Journal of Applied Polymer Science,132(35), 42503. doi:10.1002/app.42503
[13] Hamad, W. Y., & Hu, T. Q. (2010). Structure-process-yield interrelations in nanocrystalline cellulose extraction. Canadian Journal of Chemical Engineering,88(3), 392-402. doi:10.1002/cjce.20298
[14] Lloret, E., Picouet, P., & Fernández, A. (2012). Matrix effects on the antimicrobial capacity of silver based nanocomposite absorbing materials. LWT - Food Science and Technology, 49(2), 333-338. doi:http://dx.doi.org/10.1016/j.lwt.2012.01.042
[15] Rhim, J., Hong, S., & Ha, C. (2009). Tensile, water vapor barrier and antimicrobial properties of PLA/nanoclay composite films. LWT - Food Science and Technology, 42(2), 612-617. doi:http://dx.doi.org/10.1016/j.lwt.2008.02.015
[16] Sain, M., Park, S. H., Suhara, F., & Law, S. (2004). Flame retardant and mechanical properties of natural fibre–PP composites containing magnesium hydroxide. Polymer Degradation and Stability, 83(2), 363-367. doi:http://dx.doi.org/10.1016/S0141-3910(03)00280-5
[17] Sanchez-Garcia, M. D., Gimenez, E., & Lagaron, J. M. (2008). Morphology and barrier properties of solvent cast composites of thermoplastic biopolymers and purified cellulose fibers. Carbohydrate Polymers, 71(2), 235-244. doi:http://dx.doi.org/10.1016/j.carbpol.2007.05.041
[18] Singh, S. K., Sanjay, M. R., Arpitha, G. R., & Yogesha, B. (2015). 4th international conference on materials processing and characterzation study on mechanical properties of natural - glass fibre reinforced polymer hybrid composites: A review. Materials Today: Proceedings, 2(4), 2959-2967. doi:http://dx.doi.org/10.1016/j.matpr.2015.07.264
[19] Steinbuchel, A., & Heyde, M. (1998). Biodegradable polymers and macromolecules ecological considerations on the use and production of biosynthetic and synthetic biodegradable polymers. Polymer Degradation and Stability, 59(1), 3-6. doi:http://dx.doi.org/10.1016/S0141-3910(97)00017-7
[20] Steven, M. D., & Hotchkiss, J. H. (2008). Covalent immobilization of an antimicrobial peptide on poly(ethylene) film. Journal of Applied Polymer Science,110(5), 2665-2670. doi:10.1002/app.27638
[21] Sullivan, E. M., Moon, R. J., & Kalaitzidou, K. (2015). Processing and characterization of cellulose Nanocrystals/Polylactic acid nanocomposite films. Materials,8(12), 8106-8116. doi:10.3390/ma8125447
[22] Zenkiewicz, M., & Richert, J. (2008). Permeability of polylactide nanocomposite films for water vapour, oxygen and carbon dioxide. Polymer Testing, 27(7), 835-840. doi:10.1016/j.polymertesting.2008.06.005